Geology

Subducted seamounts and recent earthquakes beneath the central Cascadia forearc

Anne M. Tréhu, Richard J. Blakely and Mark C. Williams

Geology 2012;40;103-106
doi: 10.1130/G32460.1

Notes

Subducted seamounts and recent earthquakes beneath the central Cascadia forearc

Anne M. Tréhu[1], Richard J. Blakely[2], and Mark C. Williams[1]
[1]College of Oceanic and Atmospheric Sciences, Oregon State University, Corvallis, Oregon 97331-5503, USA
[2]U.S. Geological Survey, Menlo Park, California 94025-3591, USA

ABSTRACT

Bathymetry and magnetic anomalies indicate that a seamount on the Juan de Fuca plate has been subducted beneath the central Cascadia accretionary complex and is now located ~45 km landward of the deformation front. Passage of this seamount through the accretionary complex has resulted in a pattern of uplift followed by subsidence that has had a profound influence on slope morphology, gas hydrate stability, and sedimentation. Based on potential-field data and a new three-dimensional seismic velocity model, we infer that this is the most recent of several seamounts subducted over the past several million years beneath this segment of Cascadia. More deeply subducted seamounts may be responsible for recent earthquake activity on the plate boundary in this region and for along-strike variations in the thickness of the subduction channel, which may affect coupling across the plate boundary.

INTRODUCTION

The effect of seamount subduction on forearc morphology is documented from subduction zones worldwide. Subducting seamounts generally produce distinctive indentations in the deformation front as they enter the frontal prism, and their passage beneath the forearc is recorded by bathymetric furrows and a complicated pattern of uplift and subsidence (e.g., Lallemand et al., 1989; Dominguez et al., 1998). The effect on the frictional properties of the plate boundary and on generation and propagation of plate-boundary earthquakes, however, remains controversial. Relationships between plate boundary reflectivity, crustal velocity structure, and earthquake activity beneath Costa Rica (von Huene et al., 2000), Nankai (Kodaira et al., 2000; Bangs et al., 2006), northeast Japan (Mochizuki et al., 2008), and Sumatra (Singh et al., 2011) indicate that the plate boundary steps over subducting seamounts in response to high fluid pressure induced down dip of the seamount, which should reduce the normal stress on the plate boundary. Other studies, however, suggest that subducted seamounts increase the stress on the plate boundary (Scholz and Small, 1997), resulting in low-angle thrust earthquakes (Husen et al., 2002), and potentially transferring subducted seamounts to the upper plate at depths that are difficult to image seismically, as postulated by Cloos (1992). The impact of subducted seamounts on upper plate deformation, and whether and where they are transferred to the upper plate, likely varies from place to place depending on seamount size, the depth to which it has been subducted, the strength of the upper plate, and the amount of sediment on the subducting plate.

The seafloor of the Juan de Fuca plate offshore Oregon and Washington (United States) is relatively smooth west of the deformation front, and the deformation front and lower continental slope do not generally show indentations and furrows typical of subducting topography (Fig. 1; Fig. DR1 in the GSA Data Repository[1]). Based on topography observed on complementary parts of the Pacific plate, however, it is likely that many seamounts and ridges exist but are buried by the thick sediments that blanket the Juan de Fuca plate. The possible impact of these buried seamounts on subduction-zone earthquakes and segmentation along the Cascadia subduction zone has received little attention.

Although paleoseismic and historical evidence exist for very large megathrust earthquakes on the Cascadia subduction zone (e.g., Atwater et al., 2005), the instrumental record of earthquakes on the plate boundary is sparse. In 2004, two moderate earthquakes (M > 4.7) with low-angle thrust mechanisms occurred on the plate boundary near 44.5°N (Fig. 1). Since then, ~30 smaller earthquakes (M < 3.3) have occurred in this region at a rate of 3–5 events/yr; precise event relocations indicate that these

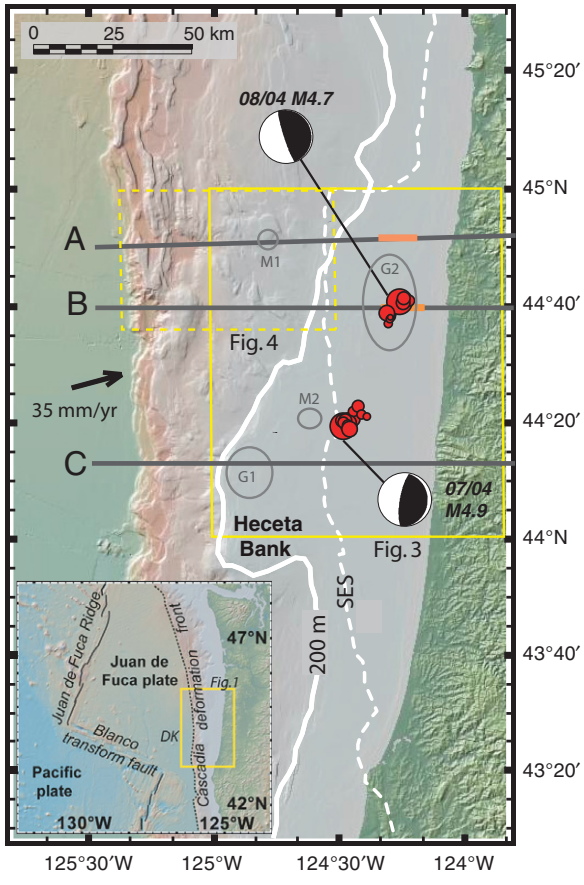

Figure 1. Topography of the central Cascadia forearc. Data from the Global Multi-Resolution Topography 2.0 synthesis (Ryan et al., 2009) accessed using GeoMapApp (www.geomapapp.org). Red dots are relocated earthquakes (Williams et al., 2011); dates, magnitudes, and mechanisms are shown for the two largest events (Tréhu et al., 2008). Slip vector shows motion of Juan de Fuca plate relative to Oregon block (McCaffrey et al., 2007). A, B, and C show locations of crustal transects in Figure 2. Orange segments in A and B indicate strong plate boundary reflectivity (Tréhu et al., 1995; Gerdom et al., 2000), which may indicate high pore pressure. Magnetic anomalies M1 and M2 and gravity anomalies G1 and G2 are shown in Figure 3 and discussed in the text. SES is seaward edge of Siletzia (see Fig. DR2 [see footnote 1]). Inset (Fig. DR1 for larger version) shows the regional setting and rough topography on the Pacific plate; DK is newly named Diebold Knoll, which rises 750 m above the generally sediment-blanketed seafloor.

[1]GSA Data Repository item 2012042, supplemental figures DR1–DR7, is available online at www.geosociety.org/pubs/ft2012.htm, or on request from editing@geosociety.org or Documents Secretary, GSA, P.O. Box 9140, Boulder, CO 80301, USA.

smaller events cluster tightly around the two larger events (Fig. 1) and define an east-dipping plane (Fig. 2). If slip heterogeneity during megathrust earthquakes is controlled by structures on the upper and lower plates, then correlations between inter-event seismicity and structure in Cascadia may provide hints about what to expect in future megathrust events.

TOPOGRAPHIC, SEISMIC, AND MAGNETIC EVIDENCE FOR A SUBDUCTED SEAMOUNT BENEATH THE CENTRAL CASCADIA ACCRETIONARY COMPLEX

Based on seismic reflection and refraction data, a 15-km-wide and 2-km-high "welt" on subducted oceanic crust beneath 8 km of sediment offshore Oregon was identified (Tréhu et al., 1994) (Fig. 2A). The welt, located ~50 km landward of the deformation front and 15 km seaward of the crystalline backstop, was interpreted to be a subducted seamount or ridge. A subtle magnetic anomaly over the welt was modeled assuming the same magnetic properties as the underlying oceanic crust (Fleming and Tréhu, 1999). The magnetic data available at the time suggested a linear structure that extended to the south; near 44°12′N it appeared to merge with a large anomaly associated with the upper plate crystalline backstop formed by Siletzia (Snavely et al., 1968). No sign of a basement ridge, however, was present in onshore and offshore large-aperture seismic data acquired in 1996 as part of the ORWELL (Oregon and Washington Exploration of the Lithosphere) project (Gerdom et al., 2000; Fig. 2B), prompting us to examine updated gravity and magnetic anomaly compilations (Figs. 3A and 3B) and extend the two-dimensional (2-D) velocity model to 3-D by inverting traveltimes from fan shots acquired along two margin-parallel lines (Fig. 3C).

Aeromagnetic data indicate that the 1989 seismic profile fortuitously passed through a circular magnetic anomaly (labeled M1 in Figs. 3B and 4A) and that several similar anomalies are present along this segment of the margin (M2–M4 in Fig. 3B; Fig. DR2), although they are dwarfed by much larger amplitude anomalies to the east and west that result from the seaward edge of Siletzia (SES) and from seafloor spreading, respectively. Similar anomalies offshore Costa Rica have been modeled as subducted seamounts (Barckhausen et al., 1998). M1 can be modeled by a cone with a height of 3.5 km and basal diameter of 5.7 km that is on top of the subducted oceanic crust, assuming a magnetic susceptibility of 0 and an east-directed remnant magnetization of 10 A/m (Fig. 4B). The summit of this cone is slightly shallower and east of the summit of the 2-D structure modeled in Fleming and Tréhu (1999). Given the nonunique nature of potential-field models and the likelihood that a subducted seamount has a more complicated geometry and internal structure, more detailed modeling is not warranted. Nevertheless, this exercise supports the conclusion that anomaly M1 and similar circular anomalies are likely caused by deeply subducted seamounts.

Seafloor morphology provides additional evidence that magnetic anomaly M1 results from a subducted seamount. We note a subtle seafloor bulge coincident with M1 and an approximately circular basin southwest of it (Fig. 4C), as would be expected if a seamount had been subducted. The basin and the bulge each have a diameter of ~10 km, and the total elevation difference between the base of the 1-km-thick basin fill and the top of the bulge is ~2.3 km (Tréhu et al., 1995), similar to the dimensions of the modeled seamount. Several low, narrow ridges cross the bulge with strikes of 324°–335°, approximately perpendicular to the relative direction of Juan de Fuca convergence (Fig. 4C). Such ridges are predicted by sandbox models of subducting conical seamounts (Dominguez et al., 1998). Northwest-trending ridges are observed elsewhere in the Cascadia accretionary complex (Fig. 1), but they tend to strike more northward or westward and are more widely spaced.

At the present convergence rate (McCaffrey et al., 2007), the seamount would have been where the basin is now ~750 k.y. ago. Although the age of sediments in the basin is unknown, depositional relationships suggest that uplift was initially to the east (Fig. DR3). As the deformation front migrated west, a new thrust ridge formed west of the basin.

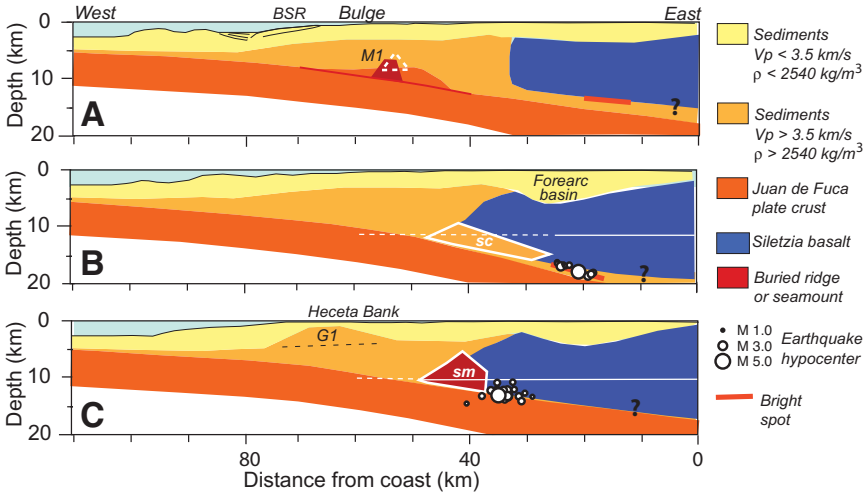

Figure 2. A: Two-dimensional (2-D) crustal model based on multichannel seismic reflection, onshore and/or offshore refraction, and potential field data (Tréhu et al., 1994, 1995; Fleming and Tréhu, 1999). Red quadrilateral is from the 2-D model of Fleming and Tréhu (1999). White dashed triangle labeled M1 is the cross section of the cone from the 3-D model in Figure 4. Locations of topographic bulge, strong bottom-simulating reflection (BSR), and slope basin interpreted to have formed in response to a subducting seamount are shown schematically with exaggerated vertical scale. SES is seaward edge of Siletzia from magnetic data. B: 2-D crustal model adapted from Gerdom et al. (2000). Region outlined in white and labeled "sc" for subduction channel is a reinterpretation of the model based on the new 3-D model (Fig. 3C). Velocity in this region is not well resolved in the 2-D model. C: Crustal model adapted from Fleming and Tréhu (1999). Region outlined in white was originally interpreted as a subducted ridge but is now interpreted to be a discrete seamount (sm) in contact with Siletzia. Region outlined in white is reinterpreted to be a discrete seamount (sm). G1 shows the excess mass needed to model gravity anomaly G1 (Fig. 3A). Hypocenters from Williams et al. (2011) are projected onto B and C with circle size proportional to magnitude. The fine horizontal white line at 11 km depth is dashed where P-wave velocity is <6 km/s, and solid where it is >6 km/s (Fig. 3C).

NEW CONSTRAINTS ON THE GEOMETRY OF THE SUBDUCTION CHANNEL

The new 3-D seismic P-wave model shows that the P-wave velocity at a depth of 11 km varies along strike (Fig. 3C; see Figs. DR4–DR7 for model details and additional depth slices). This represents the velocity immediately above the subducting plate near the SES (Fig. 2). A velocity of ~5.5 km/s north of 44°30′N is indicative of sediment subduction beneath Siletzia, whereas ~6.5 km/s to the south indicates a very thin or absent subduction channel.

Features outlined by solid white lines in Figure 2 indicate our proposed modifications to the interpretation of previously published models. These include a subduction channel a few kilometers thick beneath the outer 10–20 km of Siletzia in Figure 2B, and reinterpretation of the ridge in Figure 2C as a seamount. Resolution of the 3-D velocity model is not adequate to define the detailed geometry of the boundary between Siletzia and the seamount, but does indicate

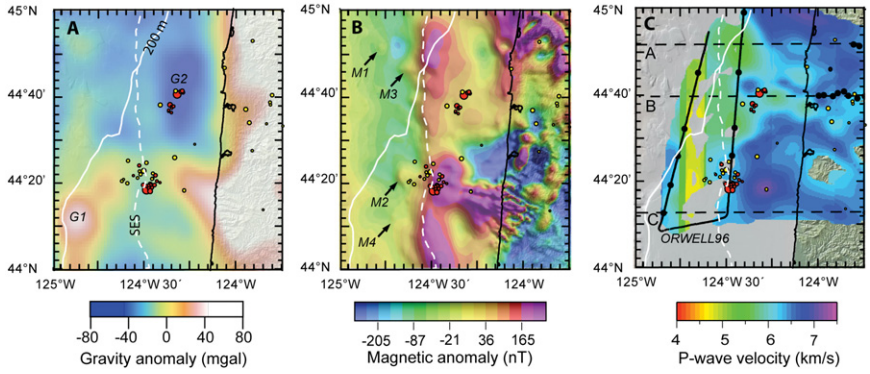

Figure 3. A: Gravity anomalies G1 and G2, discussed in the text (Sandwell and Smith v18.1 [Sandwell and Smith, 2009], accessed via GeoMapApp). SES is seaward edge of Siletzia. G1 and G2 are discussed in the text. B: Magnetic anomalies M1–M4 discussed in the text (Roberts et al., 1997). C: P-wave velocity at 11 km depth. The velocity model was determined using arrivals from margin-parallel lines of airgun shots (black line) recorded on ocean bottom and onshore seismometers (black dots). Traveltime picks were inverted using FAST (Faeroes and Shetlands Transect; Zelt and Barton, 1998); starting model was the two-dimensional (2-D) model of Gerdom et al. (2000) projected into 3-D. The model converged after 19 iterations, and the root-mean-squared traveltime misfit decreased from 0.47 s to 0.17s. Velocities are only shown for model cells sampled by ray paths. For more details, see Figures DR4–DR7 (see footnote 1). Lines labeled A, B, and C show locations of cross sections in Figure 2. Red dots in A–C represent relocated epicenters (Williams et al., 2011; see Fig. 2 for relative magnitude scale); yellow dots are epicenters of earthquakes that were not relocated because of inadequate data coverage.

either that it is attached to the subducting plate or that a subduction channel of resolvable thickness has not yet developed beneath it.

SPECULATIONS ON THE RELATIONSHIP BETWEEN SUBDUCTED SEAMOUNTS AND EARTHQUAKES

The earthquake cluster near 44°20′N, 124°25′W is located immediately west of magnetic anomaly M2 (Fig. 3B). We speculate that seismicity results from resistance to subduction as the seamount is juxtaposed against the overlying basaltic Siletz terrane. The fault plane for the 12 July 2004 earthquake is rotated 20° clockwise relative to the predicted plate motion vector (Fig. 1), possibly due to complexities in the local stress pattern as the seamount interacts with the crystalline rocks of Siletzia.

In contrast to M1, we cannot associate a simple morphological pattern on the seafloor with the projected track of M2 through the accretionary complex. M2 is currently located beneath Heceta Bank, where folded Miocene and Pliocene rocks crop out on the seafloor (Torres et al., 2009). Modeling of anomaly G1 (Fleming and Tréhu, 1999) required relatively high density material at shallow depth beneath the apparently nonmagnetic outer part of Heceta Bank (Figs. 2C and 3A). If a former subduction channel was blocked by M2 or a previously subducted seamount, the expected pattern of subsidence in the wake of the seamount may be overprinted by uplift as subducted sediments are underplated to the accretionary complex seaward of the obstruction. We note that the preferred mass excess for G1 (Fleming and Tréhu, 1999) has a cross-sectional area of ~72 km^2, which is equivalent (assuming a subduction rate of 3.5 cm/yr) to the amount of material that would back up in 450 k.y. (i.e., 16 km of subduction) if a 4-km-thick subduction channel were blocked.

The northern patch of recurrent earthquake activity, located near 44°40′N, 124°15′W and ~20 km east of the SES, is coincident with a pronounced gravity low (G2 in Fig. 3A) that corresponds to a sharp 1-km-deep, 25-km-long, and 5-km-wide depression in the Late Miocene unconformity (McNeill et al., 2000). If a subducted seamount is responsible for localized thinning of the upper plate at this location, its gravity and magnetic signature is masked by the overlying structure of the Siletzia terrane. We speculate that the basin indicated by G2 may result from a subducted seamount that was accreted to the base of the upper plate, as postulated by Cloos (1992). This should have initially caused uplift. Once it was accreted to the upper plate, the underplated material may have acted as an asperity, resulting in repeated earthquakes that gradually eroded the base of the upper plate, forming a basin (von Huene et al., 2000).

SUMMARY AND IMPLICATIONS FOR PLATE BOUNDARY COUPLING

Figure 5 summarizes our observations and compares them to the landward limit of full coupling as determined by Burgette et al. (2009) based on geodetic data. The landward limit of full coupling swings offshore between 43° and 46°N, approximately following the SES. If the clusters of recent earthquakes define the down-dip edge of strong coupling, then this boundary may be irregular, with indentations related to the history of subducted seamounts of different size and their varying impacts on the thickness of the subduction channel.

Hu and Wang (2008) showed that the strength of the upper plate influences seafloor deformation and tsunamigenesis in megathrust earthquakes. Seafloor morphology overlying and in the wake of M1 indicates a local response of the upper plate to seamount subduction. In contrast, the response of the upper plate to subduction of M2 is broadly distributed, similar to block uplift and rotation observed in Costa Rica (Gardner et al., 2001), suggesting that the strength of the upper plate varies down dip and along strike.

ACKNOWLEDGMENTS

Thanks to the many colleagues with whom we have discussed the Cascadia subduction zone over the years. This manuscript was greatly improved in response to questions from Dave Scholl, Tom Bro-

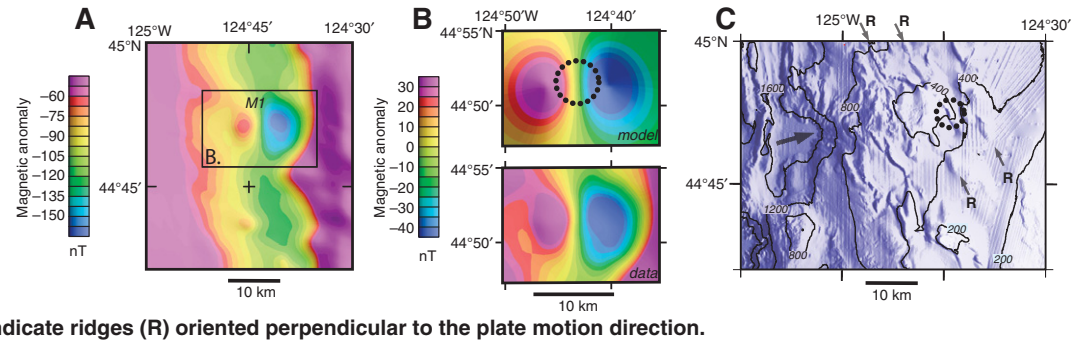

Figure 4. A: Observed magnetic anomaly data. B: Calculated anomaly (top) for a conical seamount compared to the observed anomaly (bottom) plotted with the same amplitude scale and an arbitrary reference level. See text for model parameters. C: Shaded relief showing a topographic bulge above the interpreted subducted seamount (dotted circle) and a basin in its wake. Bathymetric contours are in meters. Arrows indicate ridges (R) oriented perpendicular to the plate motion direction.

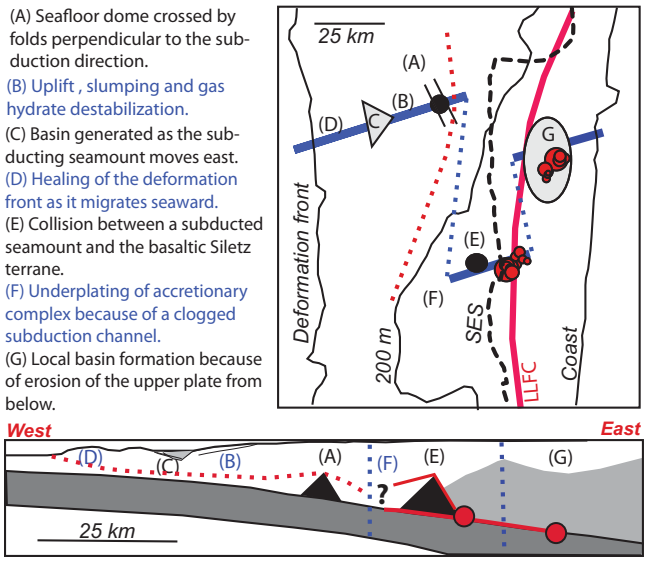

Figure 5. Schematic summary of observations and interpretations. Red circles are earthquake epicenters (see Fig. 2 caption). Blue line on map shows location of the composite cross section, with dashed segments showing discontinuities. Solid red line labeled LLFC shows the landward limit of the fully coupled plate boundary (Burgette et al., 2009). In the cross section, it shows the plate boundary where it is thought to be fully coupled; whether the current plate boundary is above or below the subducted seamount inferred from M2 (E) is not resolved with existing data. In map view, the dotted red line schematically indicates a transition in the strength of the upper plate; in cross section, it shows a portion of the plate boundary that may be weak but exhibits velocity-strengthening behavior during megathrust earthquakes (Hu and Wang, 2008). SES is seaward edge of Siletzia.

(A) Seafloor dome crossed by folds perpendicular to the subduction direction.
(B) Uplift , slumping and gas hydrate destabilization.
(C) Basin generated as the subducting seamount moves east.
(D) Healing of the deformation front as it migrates seaward.
(E) Collision between a subducted seamount and the basaltic Siletz terrane.
(F) Underplating of accretionary complex because of a clogged subduction channel.
(G) Local basin formation because of erosion of the upper plate from below.

cher, and three anonymous reviewers. The work was supported by the U.S. National Science Foundation through grants OCE-0550402 and OCE-0646226 to Oregon State University.

REFERENCES CITED

Atwater, B.F., Satoko, M.R., Satake, K., Tsuji, Y., Ueda, K., and Yamaguchi, D.K., 2005, The orphan tsunami of 1700—Japanese clues to a parent earthquake in North America: U.S. Geological Survey Professional Paper 1707, 144 p.

Bangs, N.L.B., Gulick, S.P.S., and Shipley, T.H., 2006, Seamount subduction erosion in the Nankai Trough and its potential impact on the seismogenic zone: Geology, v. 34, p. 701–704, doi:10.1130/G22451.1.

Barckhausen, U., Roeser, H.A., and von Huene, R., 1998, Magnetic signature of upper plate structures and subducting seamounts at the convergent margin off Costa Rica: Journal of Geophysical Research, v. 103, p. 7079–7093, doi:10.1029/98JB00163.

Burgette, R.J., Weldon, R.J., II, and Schmidt, D.A., 2009, Interseismic uplift rates for western Oregon and along strike variation in locking on the Cascadia subduction zone: Journal of Geophysical Research, v. 114, B01408, doi:10.1029/2008JB005679.

Cloos, M., 1992, Thrust-type subduction-zone earthquakes and seamount asperities: A physical mode for seismic rupture: Geology, v. 20, p. 601–604, doi:10.1130/0091-7613(1992)020<0601:TTSZEA>2.3.CO;2.

Dominguez, S., Lallemand, S.E., Malavieille, J., and von Huene, R., 1998, Upper plate deformation associated with seamount subduction: Tectonophysics, v. 293, p. 207–224, doi:10.1016/S0040-1951(98)00086-9.

Fleming, S., and Tréhu, A.M., 1999, Crustal structure beneath the central Oregon convergent margin from potential field modeling: Evidence for a buried basement ridge in local contact with a seaward-dipping backstop: Journal of Geophysical Research, v. 104, p. 20431–20447, doi:10.1029/1999JB900159.

Gardner, T., Marshall, J., Merritts, D., Bee, B., Burgette, R., Burton, E., Cooke, J., Kehrwald, N., Protti, M., Fisher, D., and Sak, P., 2001, Holocene forearc block rotation in response to seamount subduction, southeastern Peninsula de Nicoya, Costa Rica: Geology, v. 29, p. 151–154, doi:10.1130/0091-7613(2001)029<0151:HFBRIR>2.0.CO;2.

Gerdom, M., Tréhu, A.M., Flueh, E.R., and Klaeschen, D., 2000, The continental margin off Oregon from seismic investigations: Tectonophysics, v. 329, p. 79–97, doi:10.1016/S0040-1951(00)00190-6.

Hu, Y., and Wang, K., 2008, Coseismic strengthening of the shallow portion of the subduction fault and its effects on wedge taper: Journal of Geophysical Research, v. 113, B12411, doi:10.1029/2008JB005724.

Husen, S., Kissling, E., and Quintero, R., 2002, Tomographic evidence for a subducted seamount beneath the Gulf of Nicoya, Costa Rica: The cause of the 1990 Mw = 7.0 Gulf of Nicoya earthquake: Geophysical Research Letters, v. 29, 1238, doi:10.1029/2001GL014045.

Kodaira, S., Takahashi, N., Nakanishi, A., Miura, S., and Kaneda, Y., 2000, Subducted seamount imaged in the rupture zone of the 1946 Nankaido earthquake: Science, v. 289, p. 104–106, doi:10.1126/science.289.5476.104.

Lallemand, S., Culotta, R., and von Huene, R., 1989, Subduction of the Daiichi Kashima seamount in the Japan trench: Tectonophysics, v. 160, p. 231–247, doi:10.1016/0040-1951(89)90393-4.

McCaffrey, R., Qamar, A.I., King, R.W., Wells, R., Khazaradze, G., Williams, C.A., Stevens, C.W., Vollick, J.J., and Zwick, P.C., 2007, An update of Quaternary faults of central and eastern Oregon: Geophysical Journal International, v. 169, p. 1315–1340, doi:10.1111/j.1365-246X.2007.03371.x.

McNeill, L.C., Goldfinger, C., Kulm, L.D., and Yeats, R.S., 2000, Tectonics of the Neogene Cascadia forearc basin: Investigations of a deformed late Miocene unconformity: Geological Society of America Bulletin, v. 112, p. 1209–1224, doi:10.1130/0016-7606(2000)112<1209:TOTNCF>2.0.CO;2.

Mochizuki, K., Yamada, T., Shinohara, M., Yamanaka, Y., and Kanazawa, T., 2008, Weak interplate coupling by seamounts and repeating M~7 earthquakes: Science, v. 321, p. 1194–1197, doi:10.1126/science.1160250.

Roberts, C.W., Blakely, R.J., and Finn, C., 1997, Preliminary merged aeromagnetic map of Oregon: U.S. Geological Survey Open-File Report 97–0440, 2 sheets, scale 1:500,000, 1 table.

Ryan, W.B.F., Carbotte, S.M., Coplan, J.O., O'Hara, S., Melkonian, A., Arko, R., Weissel, R.A., Ferrini, V., Goodwillie, A., Nitsche, F., Bonczkowski, J., and Zemsky, R., 2009, Global multi-resolution topography synthesis: Geochemistry Geophysics Geosystems, v. 10, Q03014, doi:10.1029/2008GC002332.

Sandwell, D.T., and Smith, W.H.F., 2009, Global marine gravity from retracked Geosat and ERS-1 altimetry: Ridge segmentation versus spreading rate: Journal of Geophysical Research, v. 114, B01411, doi:10.1029/2008JB006008.

Scholz, C.H., and Small, C., 1997, The effect of seamount subduction on seismic coupling: Geology, v. 25, p. 487–490, doi:10.1130/0091-7613(1997)025<0487:TEOSSO>2.3.CO;2.

Singh, S., Hananto, N., Mukti, M., Robinson, D.P., Das, S., Chauhan, A., Carton, H., Gratacos, B., Midnet, S., Djajadihardha, Y., and Harjono, H., 2011, Aseismic zone and earthquake segmentation associated with a deep subducted seamount in Sumatra: Nature Geoscience, v. 4, p. 308–311, doi:10.1038/ngeo1119.

Snavely, P.D., MacLeod, N.S., and Wagner, H.C., 1968, Tholeiitic and alkalic basalts of the Eocene Siletz River Volcanics, Oregon Coast Range: American Journal of Science, v. 266, p. 454–481, doi:10.2475/ajs.266.6.454.

Torres, M.E., Embley, R.W., Merle, S.G., Tréhu, A.M., Collier, R.W., Suess, E., and Heeschen, K.U., 2009, Methane sources feeding cold seeps on the shelf and upper continental slope off central Oregon, USA: Geochemistry Geophysics Geosystems, v. 10, Q11003, doi:10.1029/2009GC002518.

Tréhu, A.M., Asudeh, I., Brocher, T.M., Luetgert, J., Mooney, W.D., Nabelek, J.L., and Nakamura, Y., 1994, Crustal architecture of the Cascadia forearc: Science, v. 266, p. 237–243, doi:10.1126/science.266.5183.237.

Tréhu, A.M., Lin, G., Maxwell, E., and Goldfinger, C., 1995, A seismic reflection profile across the Cascadia subduction zone offshore central Oregon: New constraints on the deep crustal structure and on the distribution of methane in the accretionary prism: Journal of Geophysical Research, v. 100, p. 15101–15116, doi:10.1029/95JB00240.

Tréhu, A.M., Braunmiller, J., and Nabelek, J.L., 2008, Probable low-angle thrust earthquakes on the Juan de Fuca–North America plate boundary: Geology, v. 36, p. 127–130, doi:10.1130/G24145A.1.

von Huene, R., Ranero, C.R., and Weinrebe, W., 2000, Quaternary convergent margin tectonics of Costa Rica, segmentation of the Coco Plate and central American volcanism: Tectonics, v. 19, p. 314–334, doi:10.1029/1999TC001143.

Williams, M.C., Tréhu, A.M., and Braunmiller, J., 2011, Seismicity at the Cascadia plate boundary beneath the Oregon continental shelf: Seismological Society of America Bulletin, v. 101, p. 940–950, doi:10.1785/0120100198.

Zelt, C.A., and Barton, P.J., 1998, 3-D seismic refraction tomography: A comparison of two methods applied to data from the Faeroe Basin: Journal of Geophysical Research, v. 103, p. 7187–7210, doi:10.1029/97JB03536.

Manuscript received 13 May 2011
Revised manuscript received 1 September 2011
Manuscript accepted 6 September 2011

Printed in USA